



# Histone methyltransferase Dot1L recruits O-GlcNAc transferase to target chromatin sites to regulate histone O-GlcNAcylation

Received for publication, April 10, 2022, and in revised form, May 20, 2022. Published, Papers in Press, June 9, 2022.

<https://doi.org/10.1016/j.jbc.2022.102115>

Bo Xu<sup>1</sup>, Can Zhang<sup>1</sup>, Ao Jiang<sup>1</sup>, Xianhong Zhang<sup>1</sup>, Fenfei Liang<sup>1</sup>, Xueqing Wang<sup>1</sup>, Danni Li<sup>1</sup>, Chenglong Liu<sup>1</sup>, Xiaomei Liu<sup>1</sup>, Jing Xia<sup>1</sup>, Yang Li<sup>1</sup>, Yirong Wang<sup>1</sup>, Zelan Yang<sup>1</sup>, Jia Chen<sup>1</sup>, Yu Zhou<sup>1</sup>, Liang Chen<sup>1,\*</sup>, and Hui Sun<sup>1,2,\*</sup>

From the <sup>1</sup>College of Life Sciences, Wuhan University, Wuhan, Hubei Province, China; <sup>2</sup>Hubei Province Key Laboratory of Allergy and Immunology, Wuhan University, Wuhan, Hubei Province, China

Edited by Brian Strahl

O-GlcNAc transferase (OGT) is the distinctive enzyme responsible for catalyzing O-GlcNAc addition to the serine or threonine residues of thousands of cytoplasmic and nuclear proteins involved in such basic cellular processes as DNA damage repair, RNA splicing, and transcription preinitiation and initiation complex assembly. However, the molecular mechanism by which OGT regulates gene transcription remains elusive. Using proximity labeling-based mass spectrometry, here, we searched for functional partners of OGT and identified interacting protein Dot1L, a conserved and unique histone methyltransferase known to mediate histone H3 Lys79 methylation, which is required for gene transcription, DNA damage repair, cell proliferation, and embryo development. Although this specific interaction with OGT does not regulate the enzymatic activity of Dot1L, we show that it does facilitate OGT-dependent histone O-GlcNAcylation. Moreover, we demonstrate that OGT associates with Dot1L at transcription start sites and that depleting Dot1L decreases OGT associated with chromatin globally. Notably, we also show that down-regulation of Dot1L reduces the levels of histone H2B S112 O-GlcNAcylation and histone H2B K120 ubiquitination *in vivo*, which are associated with gene transcription regulation. Taken together, these results reveal that O-GlcNAcylation of chromatin is dependent on Dot1L.

The unique and essential O-GlcNAc transferase (OGT), which is comprised of the tetratricopeptide repeat (TPR) domain and enzymatic catalyze domain (1, 2), is fundamental for mammalian cell proliferation and survival (3, 4). OGT positioned in mitochondria, cytoplasm, and nucleus can glycosylate numerous proteins by catalyzing a single O-GlcNAc linked to the serine or threonine residues (5–7). O-GlcNAcylation is implicated in a myriad of fundamental biological procedures. First, O-GlcNAcylation is presented to regulate protein stability (8, 9), interaction (10–12), and localization (13–15). Secondly, numerous studies demonstrated that O-GlcNAcylation could communicate with

ubiquitination (16–18), phosphorylation (19–23), methylation (24), and further impacted cellular processes containing gene transcription, DNA damage repair, RNA splicing, and protein translation. Thirdly, aberrant O-GlcNAcylation is usually correlated with metabolic syndrome (25–27), regulator dysfunctional (28, 29), various cancer development (30–32), and types of diseases progression (33–36).

OGT has a crucial role in gene transcriptional regulation. TBP O-GlcNAcylation impaired its assembly complex with TAFs and regulated lipid metabolism-related genes (37). The O-GlcNAcylation of RNA polymerase II on C-terminal domain (CTD) is required for the preinitiation complex assembled, and the de O-GlcNAcylation of RNA polymerase II on CTD is requisite for entrance transcription elongation (38, 39). Of note, the protein TET2 or TET3 recruited OGT to associate with HCF-1 and glycosylated it, which further promotes the gene expression by stabilizing the H3K4 methyltransferase complex integrity (40). Additionally, OGT consolidates the gene repression state by O-GlcNAcylation of chromatin silencing regulators (24).

Dot1L (Disruptor of telomeric silencing-1 like), the unique and conserved H3K79 methyltransferase, methylating lys79 of histone H3 including mono, di, and trimethylation is distributed on promoters and transcriptionally active regions (41). It has been well established that Dot1L is involved in modulating DNA damage response (42), cell proliferation and senescence (43–46), cell-fate determination (47), and numerous diseases and cancers (48–53), directly or indirectly. In addition, Dot1L is involved in transcription elongation and transcription initiation. Dot1L was associated with actively transcribing RNA polymerase II to regulate transcription elongation (54). A recent study characterized that Dot1L is implicated in the regulation of transcription initiation by facilitating the recruitment of transcription initiation factor TFIID and promoting histone H2B K120 ubiquitination (55). Interestingly, Dot1L could direct cell differentiation and control transcription elongation independent of H3K79 methylation (47).

OGT has an indispensable noncatalytic role that is required for cell proliferation, and OGT glycosylation activity is required to preserve cell viability (4). However, the fundamental question of how OGT and O-GlcNAc regulate gene expression to maintain cell viability and sustain cell

\* For correspondence: Liang Chen, [liang\\_chen@whu.edu.cn](mailto:liang_chen@whu.edu.cn); Hui Sun, [sunhui@whu.edu.cn](mailto:sunhui@whu.edu.cn).

## Dot1L regulates histone O-GlcNAcylation

proliferation has not been well defined. Therefore, identifying essential substrates and associated partners of OGT is necessary. Herein, we performed proximity labeling by coupling the efficient biotin ligase TurboID with OGT in HEK293T cells and identifying new partners of OGT. We found that Dot1L and OGT physically interact *via* the noncatalytic domain, and Dot1L positively facilitates OGT associated with chromatin to regulate histone O-GlcNAcylation.

### Results

#### The proximity-dependent method identifies the interacted proteins of OGT

Several research groups have reported many OGT interaction proteins with significant functions in different cells by proteome microarray (56), affinity purification-based mass

spectrometry (MS) (57), immunoprecipitation-based MS (17), and cross-linking-based MS (58). Recently, Branon *et al.* (59) reported TurboID-based proximity labeling MS, performed by fusion target protein with TurboID. This optimized biotin enzyme can biotinylate interaction proteins inside the native cellular environment in 10 min and has been used widely and successfully in interaction proteins identification.

Herein, we performed the TurboID-based proximity labeling MS method to identify the interacted proteins of OGT in HEK293T cells. The flow chart is shown in Figure 1A. In the quest for physiological and specific OGT-interactome, we constructed OGT-TurboID fusion protein with nuclear localization signal and Flag tag stable expression HEK293T cell line (OGT-TurboID-NLS-Flag) by lentivirus packing. Moreover, constructing TurboID fusion with nuclear localization

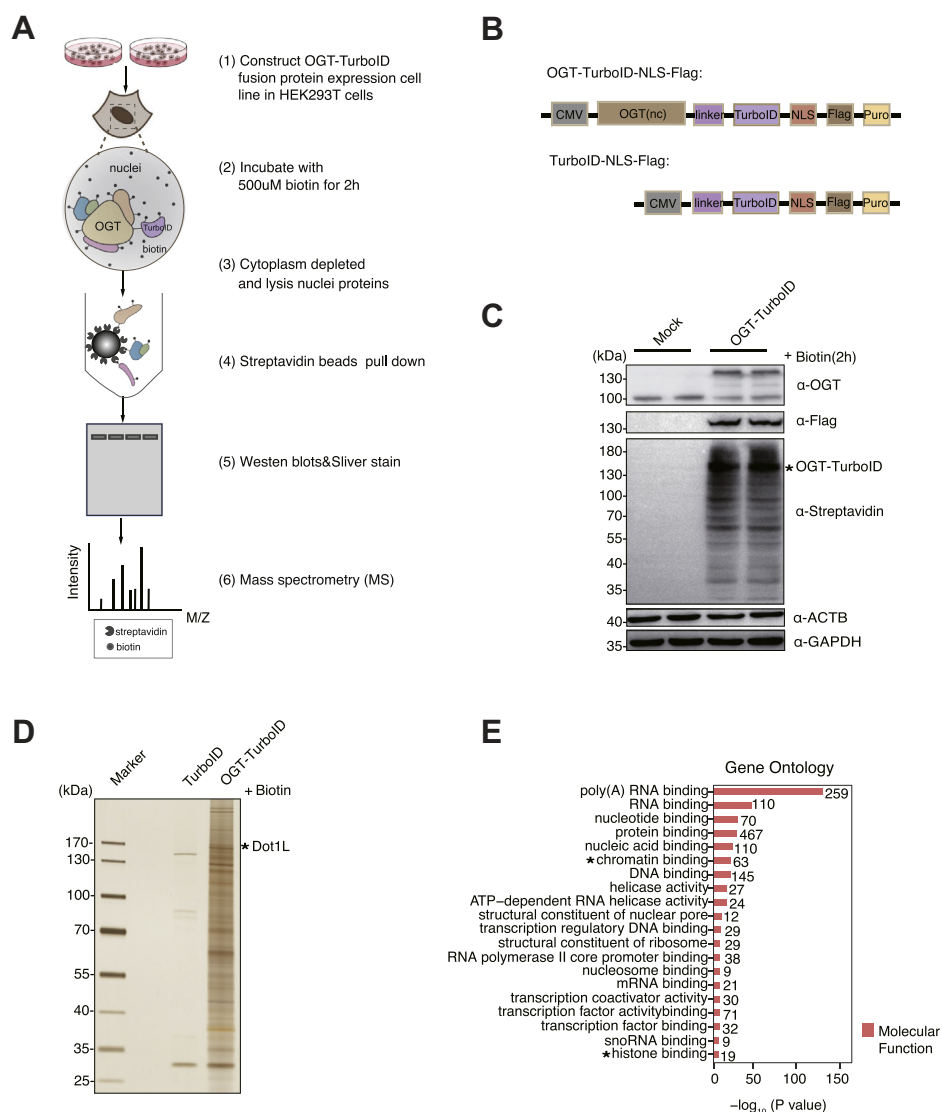


**Figure 1. The proximity-dependent method identifies the interacted proteins of OGT.** A, schematic for the process of the experiments and identification of proteins associated with OGT. B, structures of human nuclear isoform protein OGT with TurboID-NLS-Flag fusion and TurboID-NLS-Flag expression constructs. C, Western blots analysis of OGT-TurboID-NLS-Flag overexpression stable HEK293T cell lines and normal HEK293T cells (Mock) by indicated antibody in the presence or absence of biotin. Asterisks denote OGT and TurboID fusion proteins. D, silver stain of biotinylated nuclear proteins after pulldown by streptavidin beads. E, gene ontology analysis of 676 candidate proteins in OGT mass spectrometry (MS) results. OGT, O-GlcNAc transferase.

signal and Flag tag stable expression HEK293T cell line (TurboID-NLS-Flag) by lentivirus packing as control (Fig. 1B). Biotinylation was induced by incubating the biotin in cell culture media. Western blots confirmed the TurboID enzyme activity and correctly validated the fusion protein expression (Figs. 1C and S1A). Cells were labeled with biotin for 2 h, and the nuclei lysate was performed affinity purification by streptavidin beads. Proximity labeling with biotin of OGT-TurboID-NLS-Flag- and TurboID-NLS-Flag-interacted proteins presented markedly different patterns in silver stain (Fig. 1D). Proximity interactors were analyzed by MS, excluding those proteins in control.

The proteomic results (Table S1, A–C) showed that 676 unique proteins interacted with OGT (Fig. S1B). Among the 676 proteins, there are splicing factors, transcription regulators, chromatin modifiers, and histone modification enzymes. A webserver OGT-Protein Interaction Network containing 784 high-stringency human OGT interactors was recently reported by Ma *et al.* (60). Notably, 106 high-stringency OGT interactors (Table S1D) were included in OGT-TurboID interactors (Fig. S1C). Several OGT interactors, including HCFC1, HIRA, RNA polymerase II, and TRIM28, were regulated by O-GlcNAcylation, which has been described previously (24, 39, 61, 62). Dot1L, the histone methyltransferase responsible for histone H3 Lys79 H3K79 methylation, was also

recently reported as a potential OGT interactor but had not looked further into the functional roles (63). Distinct classification within OGT associated proteins showed gene ontology analysis (Fig. 1E).

**Dot1L and OGT interact with each other by noncatalyze domain**

To confirm the interaction between Dot1L and OGT, we performed coimmunoprecipitation assays with overexpressed OGT and Dot1L in several cells. We ectopically cotransfected with HA-tagged Dot1L and Flag-tagged OGT in HEK293T and HeLa S3 cells, and immunoblotting analysis with the indicated antibodies showed that Dot1L could be pulled down OGT successfully (Fig. 2A), and consistent results were observed in MCF-7 and U87MG cells (Fig. S2A). To verify whether Dot1L could pull down OGT, we transiently expressed Flag-Dot1L and HA-OGT in MCF-7, U87MG, and HeLa S3 cells, then performed immunoprecipitation by the anti-Flag affinity gel. Immunoblotting analysis confirmed that OGT was associated with Dot1L (Figs. 2B and S2B). Similarly, we ectopically expressed HA-Dot1L alone or combined with Flag-OGT or GFP-OGT in HEK293T cells, then performed immunoprecipitation by the anti-HA antibody. Flag-OGT or GFP-OGT was associated with HA-Dot1L in the reciprocal

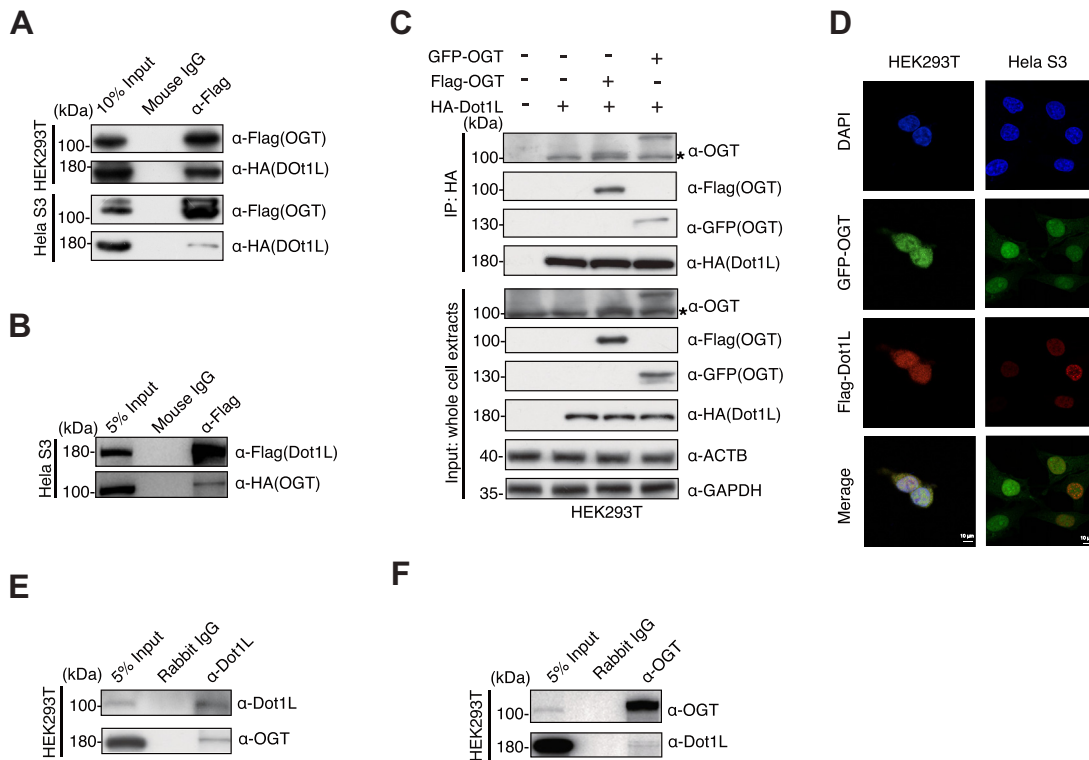


**Figure 2. Dot1L interacts with OGT.** A, Flag-OGT and HA-Dot1L were cotransfected in HEK293T cells and HeLa S3 cells and immunoprecipitated by Flag antibody and performing Western blots analysis. Mouse IgG immunoprecipitation served as a negative control. B, HA-OGT and Flag-Dot1L were cotransfected in HeLa S3 cells and immunoprecipitated by Flag antibody and performing Western blots analysis. C, HEK293T cells transient expression HA-Dot1L alone, combined with Flag-OGT or GFP-OGT. After 48 h transfection, whole-cell lysis was immunoprecipitated with HA antibody and immunoblots analysis with indicated antibodies. Asterisks denote endogenous OGT proteins. D, immunofluorescence staining of OGT and Dot1L in HEK293T cells and HeLa S3 cells were cotransient expressions of GFP-OGT and Flag-Dot1L, respectively. The scale bar represents 10 μm. E and F, nuclear lysates from HEK293T cells was subjected to immunoprecipitation with Dot1L antibody (E) and OGT antibody (F) and immunoblotting analysis with the indicated antibodies. OGT, O-GlcNAc transferase.

## Dot1L regulates histone O-GlcNAcylation

immunoprecipitation (Fig. 2C). Additionally, endogenous OGT was coimmunoprecipitated by HA-Dot1L (Fig. 2C). Immunofluorescent staining suggested a partial colocalization between Dot1L and OGT when coexpressed GFP-OGT, and Flag-Dot1L were coexpressed in HEK293T or HeLa S3 cell lines (Fig. 2D). Indeed, the physical interaction between Dot1L and OGT was further confirmed by immunoprecipitation at the endogenous protein level in HEK293T cells (Fig. 2, E and F). These results indicated that Dot1L interacts with OGT in the nucleus in different cells.

To further map the interaction regions between Dot1L and OGT, several deleted constructs were generated. The Dot1L consists of the N terminal catalyze and DNA binding region (residues 1–416) and C domain (residues 416–1537) (Fig. 3A).

To determine which subunit region of Dot1L is responsible for interaction associated with OGT, we performed immunoprecipitation and found that the C domain mediated the interaction (Figs. 3B and S3A). Further immunoprecipitation of OGT with truncated-Dot1L F3-F7 (Fig. 3C) implied that residues 416 to 816 in the C domain were responsible for the interaction of Dot1L with OGT (Fig. 3D). The OGT consists of the N terminal TPR domain (residues 1–473) and C enzymatic domain (residues 473–1046), and three TPR internal deleted truncators of OGT were constructed (Fig. 3E). Immunoprecipitation of TPR internal deletion truncated-OGT with full-length Dot1L showed a significantly decreased binding to Dot1L when TPR4–7 were deleted, suggesting that the TPR4–7 of OGT was able to mediate the interaction of OGT and

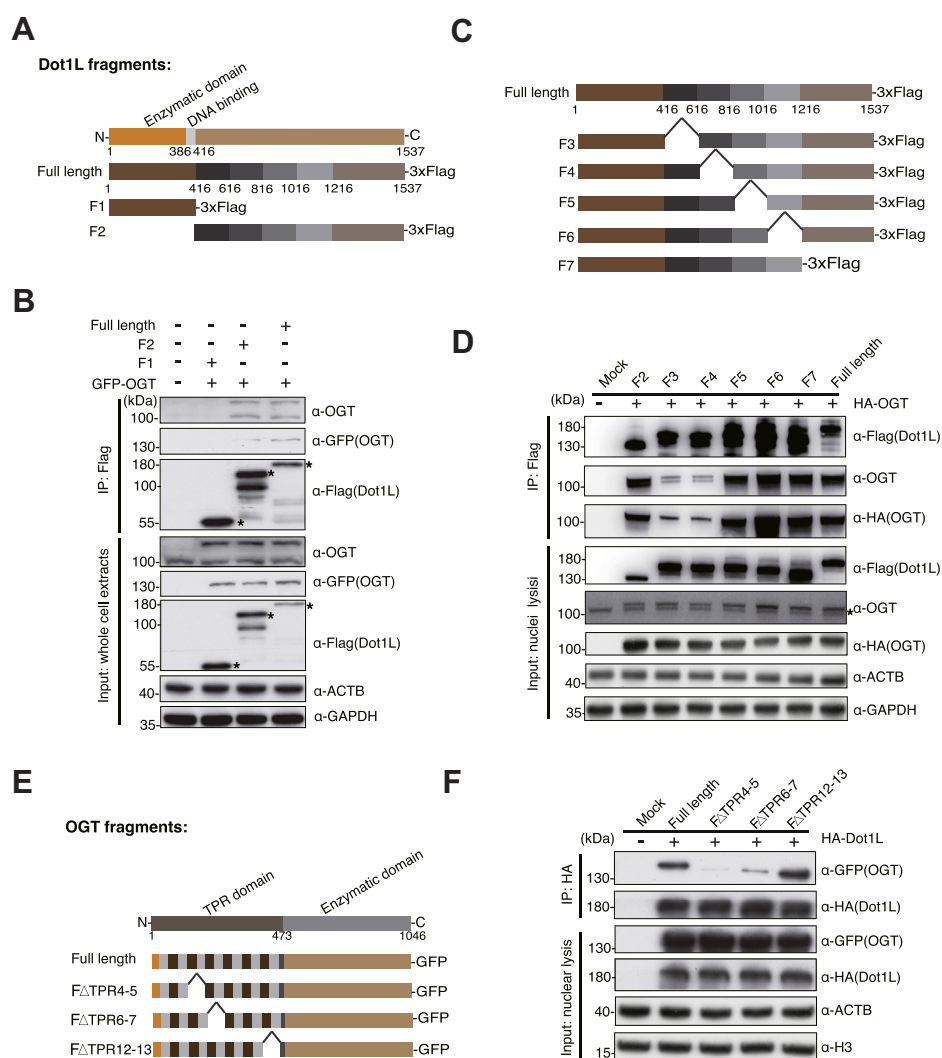


**Figure 3. Dot1L and OGT interact by noncatalyze domain.** A, schematic diagram of full-length human Dot1L and Flag-tagged N terminal of Dot1L containing the enzymatic domain and DNA-binding domain (F1) and Flag-tagged C terminal of Dot1L-containing residues 416 to 1537 (F2). B, cotransfecting GFP-OGT with full-length Dot1L, Dot1L constructs F1 and Dot1L constructs F2, in HEK293 cells, respectively. Immunoprecipitated by anti-Flag magnetic beads and analysis by Western blots with indicated antibodies. Asterisks denote the Flag-tagged Dot1L and Dot1L fragments. C, schematic diagram showing the Dot1L partial sequence-deleted fragments including F3, F4, F5, F6, and F7. D, HEK293T cells transfected HA-OGT together with full-length Dot1L, or Dot1L split F2, or F3, or F4, or F5, or F6, or F7, respectively. Nuclear lysis was subsequently immunoprecipitated by anti-Flag affinity gel and performed immunoblots with indicated antibodies. Asterisks denote endogenous OGT proteins. E, schematic diagram shows full-length human OGT, and TPR4-5 deleted GFP-tagged OGT, TPR6-7 deleted GFP-tagged OGT, and TPR12-13 deleted GFP-tagged OGT. F, HEK293T cells cotransfected HA-Dot1L with full-length GFP-OGT or TPR4-5 deleted OGT, TPR6-7 deleted OGT, or TPR12-13 deleted OGT, respectively. Nuclear lysis was applied to perform immunoprecipitation and immunoblots with indicated antibodies. OGT, O-GlcNAc transferase; TPR, tetratricopeptide repeat.

Dot1L (Fig. 3F). Collectively, these results suggested that Dot1L and OGT physically interact with each other by non-catalyze domain.

Next, we sought to determine whether Dot1L was modified by OGT. As shown in Fig. S4A, we transiently expressed Flag-Dot1L combined with OGA inhibitor Thiamet G treated in HEK293T cells, then performed immunoprecipitation by anti-Flag antibody. Immunoblotting with anti-O-GlcNAc antibodies showed that Dot1L was O-GlcNAcylated. Moreover, the O-GlcNAcylation level of Dot1L was increased when coexpressed the HA-OGT combined with the OGA inhibitor Thiamet G treated, and the O-GlcNAcylation level of Dot1L was decreased when coexpressed the Myc-OGA combined with OGT inhibitor OSMI-1 treated (Fig. S4A). These results revealed that Dot1L was O-GlcNAcylated. In addition, treating HEK293T cells with OGA inhibitor Thiamet G and immunoprecipitated the endogenous Dot1L using the anti-Dot1L antibody suggested that Dot1L was O-GlcNAcylated at the endogenous level, and the O-GlcNAcylation level was increased when HA-OGT was transiently expressed in HEK293T cells (Fig. S4B). Collectively, these results indicated that Dot1L is an O-GlcNAcylated protein.

To address whether O-GlcNAcylation of Dot1L modulates its protein stability and enzyme activity, treating HEK293T cells with OGT inhibitor OSMI-1 or OGA inhibitor Thiamet G displayed a significant effect on the whole cell lysate proteins O-GlcNAcylation (Fig. S5, A and B) but not for Dot1L's protein expression level and catalyze activity (Fig. S5, C–H). Moreover, HEK293T cells were transfected with siRNA to knock down OGT, or OGA does markedly decrease the expression of OGT and OGA (Fig. S6, A–C) but does not noticeably change the H3K79 methylation level and Dot1L protein stability (Fig. S6, C–E). These results demonstrate that although Dot1L was O-GlcNAcylated, inhibition of the enzymatic activity or deletion of OGT or OGA had exerted no distinct influence on Dot1L's protein level or enzymatic activity.

### Dot1L regulates histone O-GlcNAcylation

To investigate whether Dot1L regulates OGT, treating HEK293T cells with Dot1L inhibitor EPZ5676 does inhibit Dot1L enzymatic activity (Fig. S7A) but does not impact the OGT and OGA protein expression and enzymatic activity on nuclear proteins, cytoplasm proteins, and histone (Fig. S7, B–D). Notably, knocking down Dot1L by transfected HEK293T cells with three independent siRNA showed significantly reduced mRNA and protein levels of Dot1L (Fig. 4, A and B). Interestingly, knocking down Dot1L by siRNA slightly impacted the O-GlcNAcylation of partial nuclear proteins (Fig. S8A) but not cytoplasm proteins (Fig. S8B). Then, the histone was purified and tested for histone O-GlcNAcylation level in HEK293T cells. Western blots presented that knockdown Dot1L decreases the level of histone O-GlcNAcylation (Fig. 4, C and D). Deleting Dot1L through CRISPR interference technology (CRISPRi) (64) in HEK293T cells also showed similar effects on histone O-GlcNAcylation (Fig. 4E). In order to confirm these results,

Dot1L-knocked out K562 cells (Fig. 4F) was applied to check out the O-GlcNAc level of the nuclear proteins. Immunoblotting analyses suggested that removing Dot1L partially reduces O-GlcNAcylation of nuclear proteins (Fig. S8C), and histone O-GlcNAcylation levels decreased obviously (Fig. 4, F and G). Taken together, these results showed that Dot1L regulates histone O-GlcNAcylation.

### Deletion of Dot1L attenuates OGT associated with chromatin

Since Dot1L positively modulates histone O-GlcNAcylation independent of its activity, we hypothesized that Dot1L might regulate histone O-GlcNAcylation by affecting the distribution of OGT or OGA in nuclear. We isolated cytoplasm and nuclear fraction from HEK293T cells treated with siRNA targeting Dot1L or not and noted that there is no noticeable change in OGT's and OGA's protein levels (Fig. 5A). Consistently, similar results were observed from K562 cells in the presence and absence of Dot1L (Fig. S9A). To confirm whether Dot1L regulates OGT associated with chromatin, we performed the chromatin-binding assay as described previously (57). Deleting Dot1L in HEK293T cells decreased chromatin binding of OGT (Fig. 5, B and C). Similarly, the amount of OGT on chromatin also decreased when knocked out Dot1L in K562 cells (Fig. 5, D and E). These results suggest that abolishing Dot1L does not affect the amount of OGT and OGA in nuclear and cytoplasm but impedes OGT recruitment to chromatin.

To further verify our results, we established a Dox-induced-Flag-H3 expression cell line in HEK293T cells (Fig. S10A). Inducing Flag-tagged H3 expression with Dox and then performing immunoprecipitation by transfecting the cells with siRNA to delete Dot1L causes the decrease of OGT on chromatin (Figs. S10B and 5F). Collectively, these findings imply that Dot1L as a scaffold protein of OGT and Dot1L deleting would attenuate OGT associated with chromatin, and this results in a decreased O-GlcNAcylation of histone.

### Ablation of Dot1L decreases H2B S112 O-GlcNAcylation and H2B K120 ubiquitination

Results presented above implied that Dot1L positively regulates OGT associated with chromatin and affects histone O-GlcNAcylation. It has been described that H2B S112 O-GlcNAcylation distributes in euchromatic areas widely, and O-GlcNAcylation of histone H2B facilitates its mono-ubiquitylation (16). Here, we detect the level of H2B S112 O-GlcNAcylation and H2B K120 ubiquitination simultaneously upon Dot1L deletion with siRNA in HEK293T cells. Western blots with specified antibodies suggest that deleting Dot1L led to the reduction of H2B S112 O-GlcNAcylation and H2B K120 ubiquitination levels (Fig. 6, A–C). To further identify our results, operating CRISPRi to delete Dot1L in HEK293T cells showed that abolishment of Dot1L caused the decrease of H2B S112 O-GlcNAcylation and H2B K120 ubiquitination levels (Fig. 6, D–F). Similarly, the results observed in Dot1L knocked out in K562 cells paralleled the

## Dot1L regulates histone O-GlcNAcylation

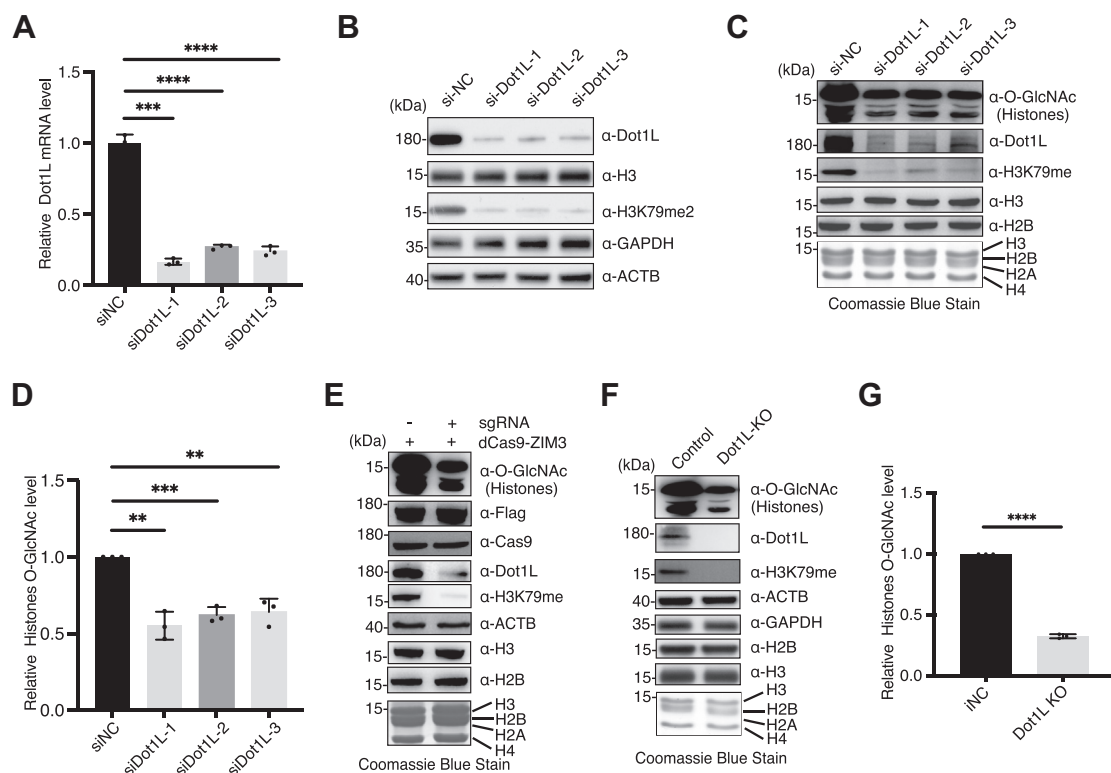


**Figure 4. Dot1L regulates histone O-GlcNAcylation.** *A*, HEK293T cells were transfected with three independent siRNA targeted Dot1L and siNC as a negative control. Quantification of the relative mRNA levels of Dot1L was carried out. Results were normalized to the expression of the gene encoding ACTB and were quantified by the change-in-threshold method ( $\Delta\Delta CT$ ). Mean  $\pm$  SEM, unpaired two-tailed *t* test, *n* = 3 biological replicates. *B*, Western blots analysis of Dot1L protein and H3K79me2 levels of *A*. *C*, deleting Dot1L in HEK293T cells with siRNA and isolating the histone. Immunoblots analysis of whole histone O-GlcNAcylation with indicated antibodies. *D*, quantification of (*C*). Mean  $\pm$  SEM, unpaired two-tailed *t* test, *n* = 3 biological replicates. *E*, HEK293T cells cotransfected with dCas9-ZIM3 and gRNA targeted the Dot1L gene promoter region to knock down Dot1L and purify the histone. Western blots detected the Dot1L, H3K79me, and histone O-GlcNAc levels with indicated antibodies. *F*, Dot1L was knocked out in K562 cells. Immunoblots analysis of Dot1L and H3K79me with indicated antibodies. Purifying histone in Dot1L knocked out K562 cells and detected the histone O-GlcNAcylation with indicated antibodies. *G*, quantification of (*F*). Mean  $\pm$  SEM, unpaired two-tailed *t* test, *n* = 3 biological replicates. Data information: \*\**p* < 0.01, \*\*\**p* < 0.001, \*\*\*\**p* < 10<sup>-4</sup> (Student's *t* test).

results in Dot1L knock down 293T cells, and both indicate that Dot1L regulates histone H2B S112 O-GlcNAcylation and H2B K120 ubiquitination (Fig. 6, *G–I*). These results directly supported that Dot1L recruited OGT to chromatin to enhance histone H2B S112 O-GlcNAcylation and promote H2B K120 ubiquitination.

### OGT is corecruited with DOT1L in HEK293T cell chromatin

Dot1L facilitates OGT associates with chromatin, which prompts us to deem that Dot1L may help OGT mediate partial substrates selected and assist OGT in regulating specific gene expression in a particular environment. To investigate this, immunoprecipitation with chromatin in HEK293T cells showed that Dot1L and OGT are coassociation with chromatin (Fig. 7A).

To systematically study the regulation between Dot1L and OGT on chromatin, we performed Dot1L and OGT Cut&Tag experiments together with high-throughput sequencing in HEK293T cells in the absence or presence of Dot1L (Fig. 7B). We first performed peak calling to check our data quality by comparing and analyzing Dot1L and OGT gene distributions and potential target genes (Table S2). Genome-wide analysis with spearman correlation heatmap revealed that OGT and

Dot1L are positively correlated with each other (Fig. 7C). Further gene distribution analysis suggested that 53.36% of Dot1L peaks were distributed in the promoter, 22.18% in the intron, 21.43% in intergenic, 1.17% in TTS, and 0.78% in exon (Fig. 7D). The proportion of OGT peaks was 54.79% distributed in the promoter, 1.49% in the intron, 20.56% in intergenic, 1.32% in TTS, and 0.62% in exon (Fig. 7E). Moreover, we detected the Cut&Tag signals at the transcription start site of the representative genes CKS1B, ANAPC15, and EIF5A (Fig. 7F). Consistent with the above, the meta-analysis also evidently displayed that OGT and Dot1L binding sites are globally concordant, mainly near the transcription start site (Fig. S11, *A* and *B*). Notably, an unexpected abundance of gene promoter-associated overlap for OGT and Dot1L (Fig. 7G) and comparable gene ontology analysis given by OGT and Dot1L (Fig. S12, *A* and *B*) reflected that potential regulation between OGT and Dot1L might exist. Therefore, we supposed that Dot1L might generally modulate OGT. To test the possibility, we performed Cut&Tag with HEK293T cells upon Dot1L knock down. Strikingly, we observed that depletion of Dot1L markedly reduced OGT associated with chromatin globally (Fig. 7H). Collectively, these results illustrated that OGT and Dot1L are coassociated with chromatin, distributed in identical patterns, and tightly correlated. Dot1L

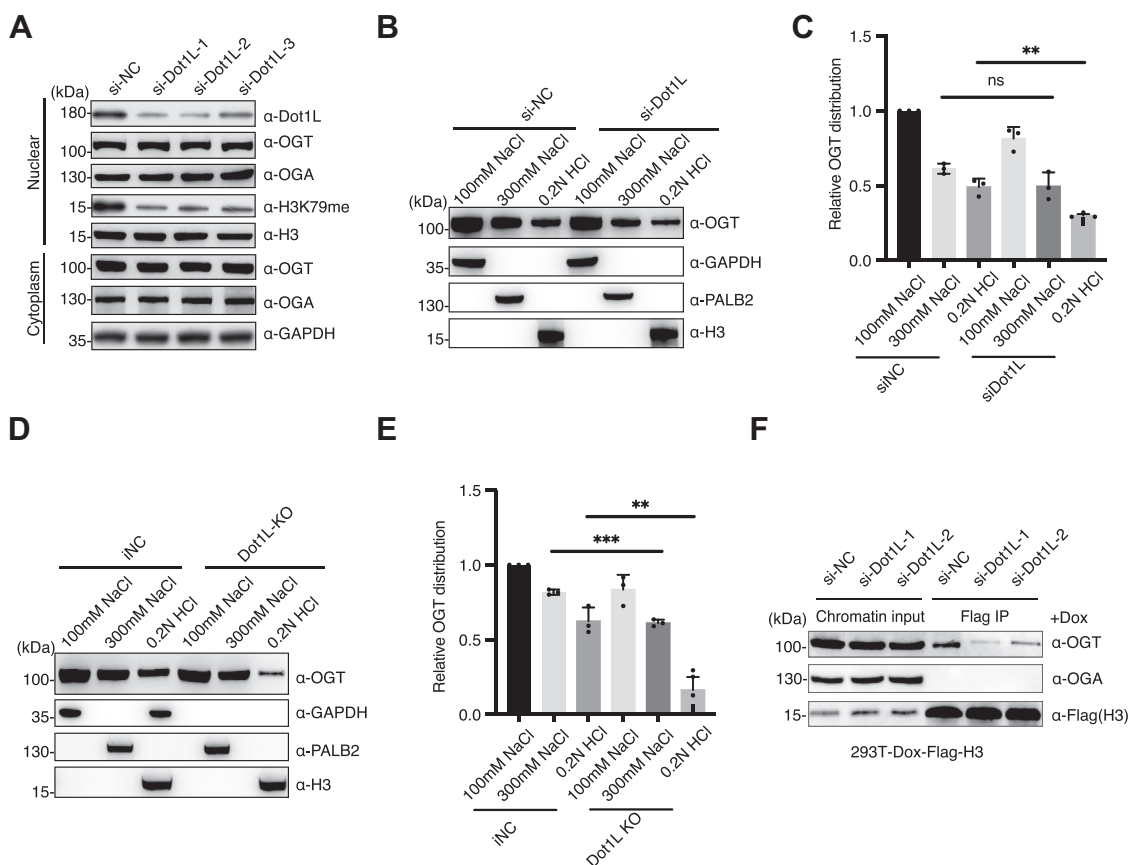


**Figure 5. Deletion of Dot1L attenuates OGT associated with chromatin.** *A*, transfecting three independent siRNA target Dot1L in HEK293T cells, siNC as a negative control. Performing nucleocytoplasmic separation and detecting the nuclear protein levels and the cytoplasm protein levels of OGT and OGA, respectively, by Western blots with indicated antibodies. *B*, HEK293T cells expressing negative control siRNA or siRNA target Dot1L performed a chromatin-binding assay to define the chromatin-associated OGT in 100 mM NaCl, 300 mM NaCl, and 0.2 N HCl, respectively. GAPDH, PALB2, and histone H3 were applied to the markers in these three different fractions. *C*, quantification of (*B*). Mean  $\pm$  SEM, unpaired two-tailed *t* test,  $n = 3$  biological replicates. *D*, operating chromatin-binding assay in the Dot1L-deleted K562 cells and control cells to detect the chromatin-associated OGT upon the deletion of Dot1L or not. *E*, quantification of (*D*). Mean  $\pm$  SEM, unpaired two-tailed *t* test,  $n = 3$  biological replicates. *F*, Dox-inducible Flag-tagged H3 stable expression HEK293T cell lines were induced Flag-H3 expression. Cells were then treated with two independent siRNA to delete Dot1L and siNC as a negative control. Isolation of chromatin and subsequently performed immunoprecipitation with anti-Flag affinity gel to detect the histone-associated OGT by Western blots. Data information: \*\* $p < 0.01$ , \*\*\* $p < 0.001$ , ns not significant (Student's *t* test). OGT, O-GlcNAc transferase.

generally regulated the association of OGT with gene promoters.

## Discussion

In this study, we have provided evidence *in vivo* that Dot1L forms complex with OGT and OGT recruited to chromatin partially depending on it. Mechanistically, the abolishment of Dot1L results in a decrease of histone O-GlcNAcylation, including histone H2B S112 O-GlcNAcylation. In addition, depletion of Dot1L also decreased histone H2B K120 ubiquitination levels. Notably, histone H2B S112 O-GlcNAcylation promotes H2B K120 ubiquitination, which is imperative for gene transcription (16). It has been well established that Dot1L activity is stimulated by histone H2B K120 ubiquitination (65, 66). Significantly, we found that Dot1L deletion would attenuate OGT access to chromatin globally, which implied that Dot1L might assist OGT to direct its substrate and target OGT to regulate gene expression. Here, we proposed a possible working model (Fig. 8) and speculated that there might be a positive feedback regulation loop in Dot1L, which recruits

OGT associated with promoting histone O-GlcNAcylation and regulating gene transcription.

## OGT may regulate gene transcription in a partner protein-dependent manner

TET2 enhances histone O-GlcNAcylation by facilitating OGT associated with chromatin (57), and AMPK negatively modulates histone H2B O-GlcNAcylation through phosphorylating OGT and further suppress OGT binding to chromatin (21). However, the protein mSin3A recruits OGT to interact with HDAC and glycosylates it, further silencing gene expression (67). The protein HCF-1, the most well-known OGT interactor, recruits OGT to modify PGC-1 $\alpha$ , which enhances PGC-1 $\alpha$  stability to facilitate gluconeogenesis (17). In addition, OGT interacts and O-GlcNAcylates HCF-1, priming the interaction of HCF-1 with ChREBP, and the O-GlcNAcylation of ChREBP is positively related to its transcriptional activity (12). CEMIP (cell migration-inducing and hyaluronan-binding protein) is the partner of OGT that promotes colorectal cancer metastasis (14). These examples proposed that

## Dot1L regulates histone O-GlcNAcylation

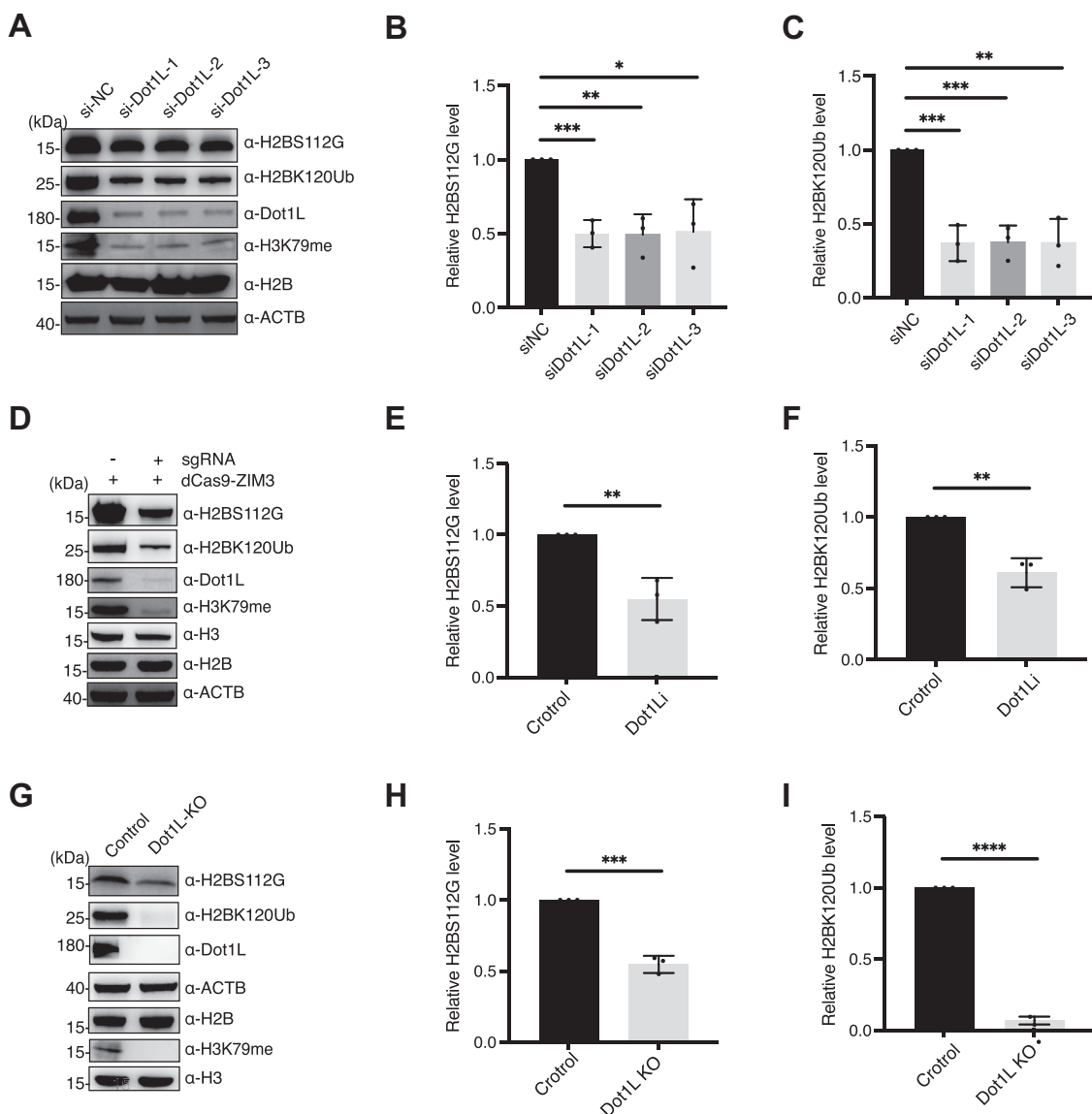


**Figure 6. Dot1L modulates H2B S112 O-GlcNAcylation and H2B K120 Ubiquitination in an OGT-dependent manner.** *A*, deleting Dot1L in HEK293T cells and purification of histone, then analyzing the H2B S112 O-GlcNAcylation levels and the H2B K120 ubiquitination levels by Western blots with indicated antibodies. *B*, quantification of the relative H2B S112 O-GlcNAcylation level of (*A*). Mean  $\pm$  SEM, unpaired two-tailed *t* test, *n* = 3 biological replicates. *C*, quantification of the relative H2B K120 ubiquitination level of (*A*). Mean  $\pm$  SEM, unpaired two-tailed *t* test, *n* = 3 biological replicates. *D*, inhibition of Dot1L in HEK293T cells and purification of histone, then analysis of the H2B S112 O-GlcNAcylation levels and the H2B K120 ubiquitination levels by Western blots with indicated antibodies. *E*, quantification of the relative H2B S112 O-GlcNAcylation level of (*D*). Mean  $\pm$  SEM, unpaired two-tailed *t* test, *n* = 3 biological replicates. *F*, quantification of the relative H2B K120 ubiquitination level of (*D*). Mean  $\pm$  SEM, unpaired two-tailed *t* test, *n* = 3 biological replicates. *G*, Dot1L knocked out K562 cells to purify histone and analyze the H2B S112 O-GlcNAcylation levels and the H2B K120 ubiquitination levels by Western blots with indicated antibodies. *H*, quantification of the relative H2B S112 O-GlcNAcylation level of (*G*). Mean  $\pm$  SEM, unpaired two-tailed *t* test, *n* = 3 biological replicates. *I*, quantification of the relative H2B K120 ubiquitination level of (*G*). Mean  $\pm$  SEM, unpaired two-tailed *t* test, *n* = 3 biological replicates. Data information: \**p*  $\leq$  0.05, \*\**p*  $<$  0.01, \*\*\**p*  $<$  0.001, \*\*\*\**p*  $<$  10<sup>-4</sup> (Student's *t* test). OGT, O-GlcNAc transferase.

the partner proteins of OGT, assisting it targets and modifying other substrates that facilitate or disrupt fundamental gene expression in some cellular processes. Numerous studies displayed here prompt us to speculate that the partner proteins of OGT may associate it with a distinct chromatin regulation complex to target different types of gene expression in specific cellular states.

Therefore, we supposed that Dot1L, as a new scaffold protein of OGT, might regulate the association of OGT with other chromatin modulators to target different genes toward the cellular state. Dot1L may assist OGT to connect basal

transcription factors or transcription machinery to regulate the transcription complex assembled and transcription cycle. Moreover, Dot1L may direct OGT attach super elongation complex to regulate transcription elongation.

### Partner proteins may help OGT to achieve substrate selection in large part

The process that OGT catalyzes countless substrates is transient in the cellular environment, which impedes the researcher from identifying and validating these interactors.

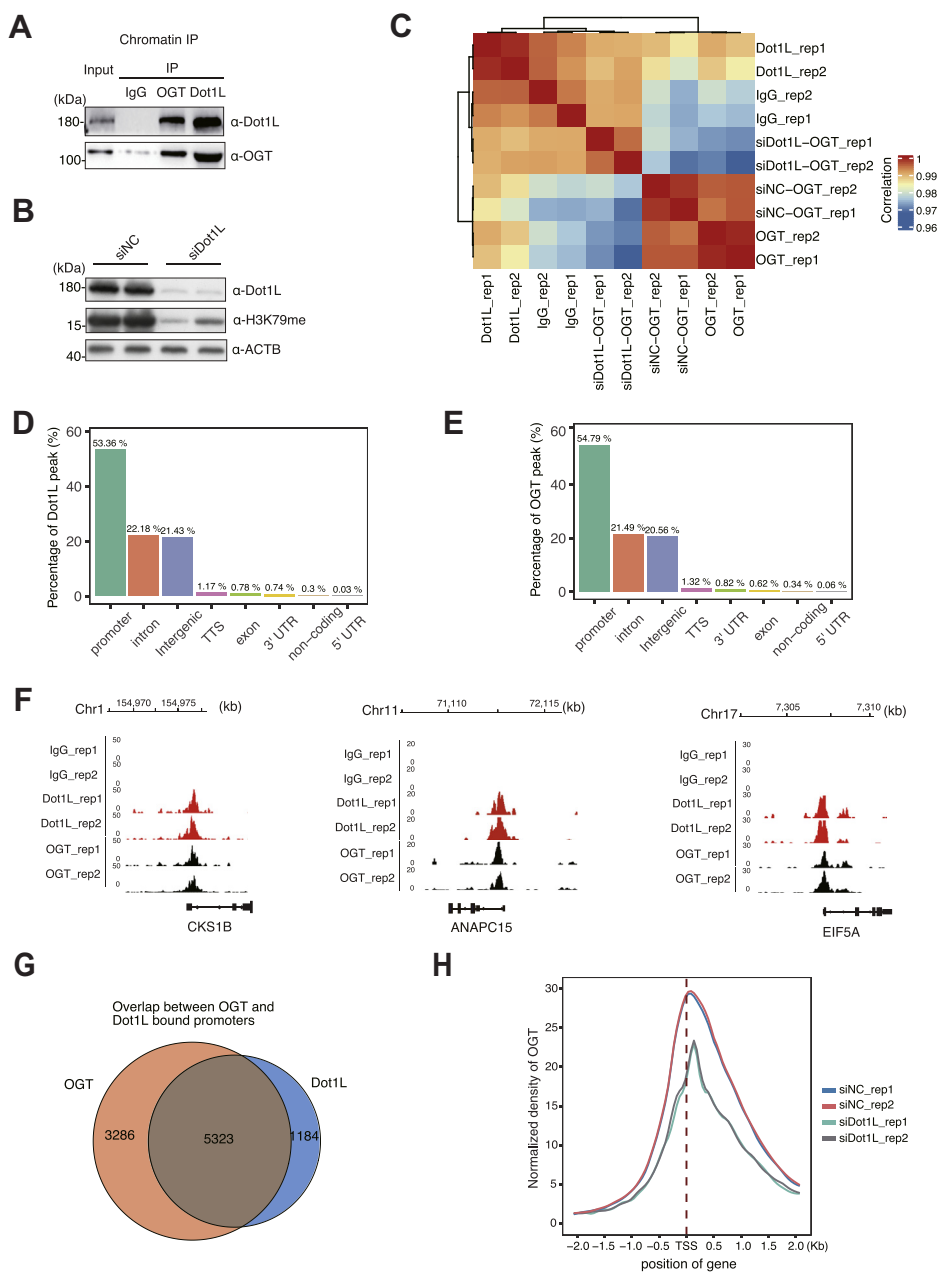


**Figure 7. Dot1L assists OGT target chromatin and regulates OGT access to chromatin.** *A*, ChIP-Western blots show the coassociation of Dot1L and OGT on chromatin in HEK293T cells. *B*, transfecting siRNA to knock down Dot1L in HEK293T cells, siNC as a negative control. *C*, Spearman correlation analysis of OGT and Dot1L Cut&Tag revealed that OGT and Dot1L are positively correlated with each other. *D* and *E*, genomic distribution of Dot1L (*D*) and OGT (*E*) Cut&Tag peaks show similar binding patterns with significant fractions mapped to gene promoters. *F*, genome browser tracks of Cut&Tag coverage at representative gene CKS1B, ANAPC15, and EIF5A. *G*, Venn diagrams of genomic association between OGT and Dot1L, implying general and functional relationships between them. *H*, metagene analysis of OGT Cut&Tag signals at the TSS in response to Dot1L deleted in HEK293T cells. OGT, O-GlcNAc transferase; TSS, transcription start site.

How OGT glycosylates thousands of substrates and regulates gene expression remains fully inclusive. Substantial studies have endeavored to define several potential mechanisms of OGT substrate selection and gene regulation. Early research involved in structure has proved that the TPR domain of OGT is intimately with substrate selectivity (68–70). Extensive efforts to the OGT interactome attract us to believe that OGT glycosylated proteins by directly regulating the TPR domain

(71, 72). Additional works pointed out that posttranslational modifications in TPR also determine its selectivity. Indeed, O-GlcNAcylation of nuclear isoform OGT and short isoform OGT in the TPR domain considerably alters the interactome (73). Similarly, phosphorylated by AMPK at threonine 444 negatively restrains OGT associated with chromatin (21). In addition, crosstalk with other posttranslational modifications shaped the substrate selection and established the platform for

## Dot1L regulates histone O-GlcNAcylation

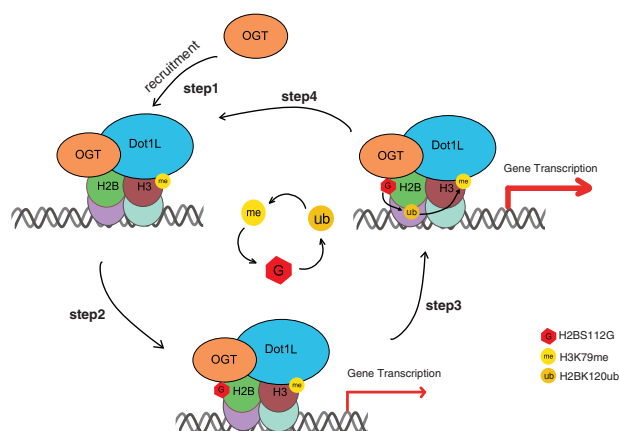


**Figure 8. A working Model for OGT regulates histone O-GlcNAcylation in a Dot1L-dependent manner.** Dot1L physical associates with OGT and assists OGT target to chromatin (step1), promoting OGT access to histone and enhancing histone O-GlcNAcylation including histone H2B S112 O-GlcNAcylation (step2). Next, GlcNAcylation of histone H2B in the S112 site facilitates histone H2B K120 monoubiquitylation, which was supposed to be positively correlated with transcriptional elongation (step3). It has been well demonstrated that H2B K120 monoubiquitylation stimulates Dot1L activity, which methylates histone H3K79, a hallmark of most actively transcribed genes (step4). Therefore, we proposed that Dot1L recruits OGT to chromatin coordinated with GlcNAcylation, ubiquitination, and methylation to modulate gene transcription. We speculated that there might be a positive feedback regulation loop in certain cellular states. OGT, O-GlcNAc transferase.

gene expression regulation. OGT was recruited to methylated promoters and O-GlcNAcylation multiple chromatin modifiers, which is a prerequisite for silencing of gene expression (24).

Directing the OGT to substrates with the help of a scaffold partner may also help to elucidate it. Indeed, depleting the protein MYPT1 decreases partial protein O-GlcNAcylation, and coexpression of the protein Sp1 with OGT prompts more glycosylated bacterial proteins confirming that MYPT1 and Sp1 are the partner proteins assisting OGT in substrate selection (71, 74). Hence, partner proteins of OGT probably play a vital role in mediating OGT substrate selection and the regulation of gene expression. To insulate the fundamental mechanism of OGT in selecting the substrates and regulating gene expression, future research focused on identifying more new scaffold proteins of OGT, especially chromatin partners, would be beneficial to understand.

## Experimental procedures

### Cell lines and cell culture

HEK293T cells, HeLa S3 cells, MCF-7 cells, U87MG cells, K562 cells, and THP-1 cells were cultured with Dulbecco's modified Eagle's media (Gibco, C11995500BT) or Roswell Park Memorial Institute 1640 Medium (Gibco, C11875500BT) supplemented with 10% fetal bovine serum (Gibco, 10099141) and 1× penicillin-streptomycin (Gibco, 15140122) at 5% CO<sub>2</sub> at 37 °C. *Mycoplasma* was detected in all cell lines.

### Reagent treatment

HEK293T cells were treated by PUGNAc (Sigma, A7229) or OSMI-1 (Abcam, ab235455) 48 h with the concentration of 10

μM, 25 μM, 50 μM to inhibit the enzyme activity of OGA or OGT, respectively. To inhibit Dot1L activity in HEK293T cells, a final concentration of 20 μM EPZ5676 (Selleck, S7079) or 20 μM SGC0946 (Selleck, S7062) was added. Two microgram/milliliter Doxycycline Hyclate (Yeasen, 60204ES03) was treated in Dox-induced Flag-H3 293T stable cell line to induce Flag-tagged H3 expression.

## Antibodies

The following antibodies were used in this study: Mouse anti-O-GlcNAc (CTD110.6, Cell Signaling Technology, #9875), Mouse anti-O-GlcNAc (CTD110.6, Santa Cruz Biotechnology, #sc-59623), Rabbit anti-OGT (Proteintech, #11576-2-AP), Mouse anti-OGT (Proteintech, #66823-1-Ig), Rabbit anti-OGT (Abcam, #ab96718), Rabbit anti-OGA (Proteintech, #14711-1-AP), Rabbit anti-Dot1L (Cell Signaling Technology, #77087), Rabbit anti-Dot1L (ZEN BIO, #R26940), Rabbit anti-H3K79me (Abcam, #ab177185), Rabbit anti-H3K79me1 (Abclonal, #A2367), Rabbit anti-H3K79me2 (Abclonal, #A2368), Rabbit anti-H3K79me3 (Abcam, #ab3594), Rabbit anti-H3K79me3 (Abclonal, #A2369), Rabbit anti-ACTB (Abclonal, #AC026), Rabbit anti-GAPDH (Abclonal, #A19056), Mouse anti-Tubulin (Santa Cruz Biotechnology, #sc-5274), Rabbit anti-PALB2 (Abclonal, #A8373), Streptavidin-HRP (Proteintech, #SA00001-0), Rabbit anti-H3 (Abclonal, #A2352), Rabbit anti-H2B (Proteintech, #15857-1-AP), Rabbit anti-GFP (Proteintech, #50430-2-AP), Mouse anti-Flag(Sigma, #F1804), Mouse anti-Flag M2 Affinity Gel (Sigma, #A2220), Mouse anti-Flag M2 Magnetic Beads (Sigma, #M8823), Mouse anti-HA (Abclonal, #AE008), Rabbit anti-H2BS112G (Abcam, #ab130951), Mouse anti-H2BK120Ub (Active Motif, #39624), Rabbit IgG (Abcam, ab171870), Alexa Fluor 594-conjugated Goat Anti-Rabbit IgG (Abclonal, AS039), Rabbit anti-Myc (Proteintech, # 16286-1-AP), and Alpaca anti-mouse IgG (NBIolab, #NBI02H).

## Plasmid, transfection, and stable cell line generation

OGT, OGA, and Dot1L coding region were amplified by the Q5 Hot Start High-Fidelity DNA polymerase (NEB, #M0515 L) and then cloned into the pLenti CMV GFP Puro vector (Addgene #17448) with restriction enzymes BamHI and Sall to produce the plasmid by Gibson assembly. Similarly, the truncated-Dot1L and truncated-OGT were created. The TurboID-coding region was amplified from the V5-TurboID-NES\_pCDNA3 vector (Addgene #107169), and then fusion constructs with OGT and cloned into the pLenti CMV GFP Puro vector by Gibson assembly. The dCas9 and ZIM3 coding regions were amplified from the pLX303-ZIM3-KRAB-dCas9 vector (Addgene #154472) and cloned into the pLenti CMV GFP Puro vector by Gibson assembly. gRNA sequence target Dot1L promoter was synthesized and cloned into the pLX-sgRNA vector (Addgene #50662). DNA and siRNA were transfected with lipofectamine 2000 (Invitrogen, 11668019) and lipofectamine RNAiMAX (Invitrogen, 13778150), respectively, according to manufacturer's instruction. Lentivirus was produced by transiently cotransfecting interesting constructs,

pMD2.G (Addgene #12259) and PSPAX2 (Addgene #12260), at the ratio of 2:2:1 in HEK293T cells. Stable cell lines were generated by lentivirus infection.

### **Coimmunoprecipitation, Western blots, and histone purification**

Cells were lysed with precold IP buffer (25 mM Tris pH 7.5, 150 mM NaCl, 1 mM EDTA, 1% NP-40, 5% glycerol, 1× protease inhibitor cocktail) and incubated with indicated antibodies rotating at 4 °C for 12 h, and 50 µl protein magnetic beads were added to each sample rotating at 4 °C for an additional 2.5 h. The beads were washed by cell lysis buffer three times and the proteins were eluted by 5× SDS loading buffer with a 10 min boil. SDS-PAGE analysis was carried out with indicated antibodies. For immunoblots only, cells were lysed with precold cell lysis buffer (50 mM Tris pH 8.0, 150 mM NaCl, 1 mM EDTA, 1% NP-40, 0.5% sodium deoxycholate, 0.1% SDS, 1× protease inhibitor cocktail) and qualifying the protein by BCA and analysis by SDS-PAGE with indicated antibodies. For histone purification, cells were lysed with precold hypotonic lysis buffer (10 mM Tris pH 8.0, 1 mM KCl, 1.5 mM MgCl<sub>2</sub>, and 1 mM DTT) and incubated for 30 min rotating at 4 °C, and lysis the intact nuclei with 0.4 N H<sub>2</sub>SO<sub>4</sub> overnight at 4 °C and precipitate the histone by TCA. Analysis of the histone was carried out by Coomassie blue staining and Western blots.

### **RNAi, CRISPRi, and RT-qPCR**

For gene knock down with siRNA, cells were transfected with indicated siRNA and harvested at 72 h after transfection. Total RNA was extracted with TRIzol reagent (Invitrogen, 10296010) in accordance with the manufacturer's instructions. Complementary DNA was synthesized by using cDNA Synthesis kit (Yeasen, 11123ES10) following manufacturer's directions. Quantitative real-time PCR was performed by using Hieff qPCR SYBR Green Master Mix (Yeasen, 11211ES03) on the BioRad CFX96 following manufacturer's protocols. For performing CRISPRi, cells were cotransfected with the vector of expression dcas9-zim3 and sgRNA-targeted Dot1L promoter and subsequently detected by Western blots with indicated antibodies. The siRNA oligonucleotide sequences (purchased from GenePharma) targeted OGT, OGA, and Dot1L which are as follows: siDot1L1 = a + b, siDot1L2 = c + d, and siDot1L3 = e + f.

### **Immunofluorescence staining**

HEK293T cells and HeLa S3 cells were cotransfected with GFP-OGT and Flag-Dot1L, and after 12 h, transfection cells were seeded on Poly-L-Lysine-coated coverslips in a 24-well culture plate. The following 24 h, cells were washed three times by 1× PBS and fixed with 4% paraformaldehyde at room temperature for 10 min. The cells were washed three times with 1× PBS and the cells were permeated by 1% Triton X-100 in PBS for 15 min at room temperature and blocking the cells with 5% bovine serum albumin and 0.5% Tween in PBS for 1 h at room temperature. Incubating cells with the Flag antibody (Sigma, F1804), washing three times with 1× TBST, and then incubating

with Alexa Fluor conjugated secondary antibodies (Abclonal, AS039) and washing three times with 1× TBST. The Nuclei were then stained with 8 µg/ml diamidino-2-phenylindole (Thermo, D1306) for 10 min at room temperature. After three times washing by 1× TBST, the slides were detected by a Leica SP8 confocal laser scanning microscope (Leica).

### **Proximity-labeling MS**

The stable OGT-TurboID-NLS-Flag cell line and stable TurboID-NLS-Flag cell line were incubated with 500 µM biotin, 5 mM MgCl<sub>2</sub>, and 1 mM ATP for 2 h. The cells were harvested and washed with precold 1× PBS three times and cytoplasm fraction was removed and the nuclei were lysed by Lysis buffer (50 mM Tris pH 8.0, 150 mM NaCl, 1 mM EDTA, 1% NP-40, 0.5% sodium deoxycholate, 0.1% SDS, 5% glycerol, 1× protease inhibitor cocktail). To maximum reduce the nonspecific proteins, block the streptavidin C1 beads (Thermo, 65002) with HEK293T nuclei fraction protein lysis and incubate the nuclei lysis with 200 µl of each sample of the streptavidin C1 beads with a rotator at 4 °C overnight. Then washing three times with Lysis buffer, one time with 1 M KCl, two times with buffer A (2 M NaCl, 10 mM Tris pH 7.5), two times with buffer B (2 M Urea, 10 mM Tris pH 8.0), one time with 0.1 M Na<sub>2</sub>CO<sub>3</sub>, one time with 10% SDS, and three times with Lysis buffer. For further analysis, 20% of the beads were eluted by 5X SDS loading buffer with a 10 min boil and then performing sliver stain assay, and 80% of the beads were used for MS analysis.

### **Chromatin isolation and chromatin-binding assay**

For chromatin isolation, cells were washed with pre-cold 1× PBS three times, lysis by Cytoplasmic lysis buffer (0.15% NP-40, 10 mM Tris-HCl pH 7.0, 150 mM NaCl) was carried out, then the cell lysate was layered onto sucrose buffer (10 mM Tris-HCl pH 7.0, 150 mM NaCl, 25% sucrose), the cytoplasm was removed and the nuclei were washed with Nuclei wash buffer (0.1% Triton X-100, 1 mM EDTA, in 1× PBS) three times, the nuclei were resuspended with Glycerol buffer (20 mM Tris pH 7.5, 75 mM NaCl, 0.5 mM EDTA, 50% glycerol, 0.85 mM DTT), then mixing with the same volume of nuclei lysis buffer (1% NP-40, 20 mM Hepes pH 7.5, 300 mM NaCl, 1 M urea, 0.2 mM EDTA, 1 mM DTT), and the supernatant was removed completely. The chromatin was resuspended and subsequent analysis was performed. For the chromatin-binding assay, cell pellets were lysed with NETN100 buffer (50 mM Tris-HCl, pH 7.4, 2 mM EDTA and 100 mM NaCl). After centrifugation, the supernatants were named 100 mM NaCl samples. The insoluble pellets were collected, washed with ice-cold PBS, and incubated with 400 ml NETN300 buffer (50 mM Tris-HCl, pH 7.4, 2 mM EDTA and 300 mM NaCl) on ice. After centrifugation, the supernatants were named 300 mM NaCl samples. The remaining pellets were washed twice with ice-cold PBS and then treated with 200 ml 0.2 N HCl. The supernatants were neutralized with 200 ml Tris-HCl, pH 8.8 and named as 0.2 N HCl fractions. All fractions were

## Dot1L regulates histone O-GlcNAcylation

subsequently performed SDS-PAGE and analysis by Western blots with indicated antibodies.

### Cut&Tag and data analysis

Cut&Tag experiments were performed at the endogenous protein level with Hieff In-Situ DNA Binding Profiling Library Prep Kit (Yeasen, 12598ES48) following the manufacturer's protocols. Briefly, for each sample,  $5 \times 10^4$  HEK293T cells were harvested and washed three times by PBS, resuspended the cells with cell wash buffer gently, and incubated with the concanavalin A coated magnetic beads previously washed by ConA bind buffer. Then, concanavalin A beads coupled cells were collected and incubated with primary antibody Rabbit IgG (Abcam, ab171870) or Dot1L (CST, 77087) or OGT (Proteintech, 11576-2-AP) at 4 °C overnight. Incubate the secondary antibody with the concanavalin A beads coupled cells at room temperature for 1 h. The ConA beads coupled cells were collected and the pA/G-Transposome Mix was added. And standard tagmentation and amplification were performed. Amplified DNA libraries were purified and shipped for next-generation sequencing. Cut&Tag data analysis was performed as described previously (75).

### Data availability

All data are available upon request. Sequences of siRNAs, guide RNAs, and primer oligonucleotides are provided in the "Primer and Sequence Table" in supporting information. The Cut&Tag data generated in this study are available in the NCBI Gene Expression Omnibus repository under accession number GSE200059 (<https://www.ncbi.nlm.nih.gov/geo/query/acc.cgi?acc=GSE200059>).

**Supporting information**—This article contains supporting information.

**Acknowledgments**—We thank Prof. Jiahui Han from Xiamen University for providing the cDNA of OGT and OGA. We thank Prof. Ming Yu from Shanghai Jiao Tong University and Prof. Qiang Chen from Wuhan University for materials support. We are grateful to Prof. Gerald Hart from University of Georgia Athens for anti-O-GlcNAc antibody support. This work was supported by the National Natural Science Foundation of China (31370849 and 31970619). The numerical calculations in this article have been done on the supercomputing system in the Supercomputing Center of Wuhan University.

**Author contributions**—L. C. and H. S. conceptualization; L. C. and H. S. supervision; L. C. and H. S. project administration; L. C. and H. S. funding acquisition; L. C. and H. S. writing—review and editing; B. X., X. Z., and Y. Z. resources; B. X. data curation; B. X., F. L., and X. W. formal analysis; B. X. and A. J. methodology; B. X., A. J., D. L., C. L., X. L., J. X., Y. L., Y. W., Z. Y., and J. C. visualization; C. Z. and X. Z. software.

**Conflict of interest**—The authors declare that they have no conflicts of interest with the contents of this article.

**Abbreviations**—The abbreviations used are: CRISPRi, CRISPR interference technology; CTD, C-terminal domain; MS, mass

spectrometry; OGT, O-GlcNAc transferase; TPR, tetratricopeptide repeat.

### References

1. Kreppel, L. K., Blomberg, M. A., and Hart, G. W. (1997) Dynamic glycosylation of nuclear and cytosolic proteins. Cloning and characterization of a unique O-GlcNAc transferase with multiple tetratricopeptide repeats. *J. Biol. Chem.* **272**, 9308–9315
2. Lazarus, M. B., Nam, Y., Jiang, J., Sliz, P., and Walker, S. (2011) Structure of human O-GlcNAc transferase and its complex with a peptide substrate. *Nature* **469**, 564–567
3. Levine, Z. G., and Walker, S. (2016) The biochemistry of O-GlcNAc transferase: which functions make it essential in mammalian cells? *Annu. Rev. Biochem.* **85**, 631–657
4. Levine, Z. G., Potter, S. C., Joiner, C. M., Fei, G. Q., Nabet, B., Sonnett, M., et al. (2021) Mammalian cell proliferation requires noncatalytic functions of O-GlcNAc transferase. *Proc. Natl. Acad. Sci. U. S. A.* **118**, e2016778118
5. Lubas, W. A., and Hanover, J. A. (2000) Functional expression of O-linked GlcNAc transferase. Domain structure and substrate specificity. *J. Biol. Chem.* **275**, 10983–10988
6. Love, D. C., Kochan, J., Cathey, R. L., Shin, S.-H., Hanover, J. A., and Kochran, J. (2003) Mitochondrial and nucleocytoplasmic targeting of O-linked GlcNAc transferase. *J. Cell Sci.* **116**, 647–654
7. Hart, G. W., Housley, M. P., and Slawson, C. (2007) Cycling of O-linked beta-N-acetylglucosamine on nucleocytoplasmic proteins. *Nature* **446**, 1017–1022
8. Chu, C. S., Lo, P. W., Yeh, Y. H., Hsu, P. H., Peng, S. H., Teng, Y. C., et al. (2014) O-GlcNAcylation regulates EZH2 protein stability and function. *Proc. Natl. Acad. Sci. U. S. A.* **111**, 1355–1360
9. Duan, F., Wu, H., Jia, D., Wu, W., Ren, S., Wang, L., et al. (2018) O-GlcNAcylation of RACK1 promotes hepatocellular carcinogenesis. *J. Hepatol.* **68**, 1191–1202
10. Ferrer, C. M., Lynch, T. P., Sodi, V. L., Falcone, J. N., Schwab, L. P., Peacock, D. L., et al. (2014) O-GlcNAcylation regulates cancer metabolism and survival stress signaling via regulation of the HIF-1 pathway. *Mol. Cell* **54**, 820–831
11. Peng, C., Zhu, Y., Zhang, W., Liao, Q., Chen, Y., Zhao, X., et al. (2017) Regulation of the Hippo-YAP pathway by glucose sensor O-GlcNAcylation. *Mol. Cell* **68**, 591–604.e5
12. Lane, E. A., Choi, D. W., Garcia-Haro, L., Levine, Z. G., Tedoldi, M., Walker, S., et al. (2019) HCF-1 regulates de novo lipogenesis through a nutrient-sensitive complex with ChREBP. *Mol. Cell* **75**, 357–371.e7
13. Tan, W., Jiang, P., Zhang, W., Hu, Z., Lin, S., Chen, L., et al. (2021) Posttranscriptional regulation of de novo lipogenesis by glucose-induced O-GlcNAcylation. *Mol. Cell* **81**, 1890–1904.e7
14. Hua, Q., Zhang, B., Xu, G., Wang, L., Wang, H., Lin, Z., et al. (2021) CEMIP, a novel adaptor protein of OGT, promotes colorectal cancer metastasis through glutamine metabolic reprogramming via reciprocal regulation of  $\beta$ -catenin. *Oncogene* **40**, 6443–6455
15. Mathew, M. P., Abramowitz, L. K., Donaldson, J. G., and Hanover, J. A. (2022) Nutrient-responsive O-GlcNAcylation dynamically modulates the secretion of glycan-binding protein galectin 3. *J. Biol. Chem.* **298**, 101743
16. Fujiki, R., Hashiba, W., Sekine, H., Yokoyama, A., Chikanishi, T., Ito, S., et al. (2011) GlcNAcylation of histone H2B facilitates its mono-ubiquitination. *Nature* **480**, 557–560
17. Ruan, H.-B., Han, X., Li, M.-D., Singh, J. P., Qian, K., Azarhoush, S., et al. (2012) O-GlcNAc transferase/host cell factor C1 complex regulates gluconeogenesis by modulating PGC-1 $\alpha$  stability. *Cell Metab.* **16**, 226–237
18. Chu, Y., Jiang, M., Wu, N., Xu, B., Li, W., Liu, H., et al. (2020) O-GlcNAcylation of SIX1 enhances its stability and promotes hepatocellular carcinoma proliferation. *Theranostics* **10**, 9830–9842
19. Yang, W. H., Kim, J. E., Nam, H. W., Ju, J. W., Kim, H. S., Kim, Y. S., et al. (2006) Modification of p53 with O-linked N-acetylglucosamine regulates p53 activity and stability. *Nat. Cell Biol.* **8**, 1074–1083
20. Hart, G. W., Slawson, C., Ramirez-Correa, G., and Lagerlof, O. (2011) Cross talk between O-GlcNAcylation and phosphorylation: roles in

- signaling, transcription, and chronic disease. *Annu. Rev. Biochem.* **80**, 825–858
21. Xu, Q., Yang, C., Du, Y., Chen, Y., Liu, H., Deng, M., *et al.* (2014) AMPK regulates histone H2B O-GlcNAcylation. *Nucleic Acids Res.* **42**, 5594–5604
  22. Freund, P., Kerenyi, M. A., Hager, M., Wagner, T., Wingelhofer, B., Pham, H. T. T., *et al.* (2017) O-GlcNAcylation of STAT5 controls tyrosine phosphorylation and oncogenic transcription in STAT5-dependent malignancies. *Leukemia* **31**, 2132–2142
  23. Park, J., Ha, H.-J., Chung, E. S., Baek, S. H., Cho, Y., Kim, H. K., *et al.* (2021) GlcNAcylation ameliorates the pathological manifestations of Alzheimer's disease by inhibiting necroptosis. *Sci. Adv.* **7**, eabd3207
  24. Boulard, M., Rucli, S., Edwards, J. R., and Bestor, T. H. (2020) Methylation-directed glycosylation of chromatin factors represses retrotransposon promoters. *Proc. Natl. Acad. Sci. U. S. A.* **117**, 14292–14298
  25. Ruan, H. B., Dietrich, M. O., Liu, Z. W., Zimmer, M. R., Li, M. D., Singh, J. P., *et al.* (2014) O-GlcNAc transferase enables AgRP neurons to suppress browning of white fat. *Cell* **159**, 306–317
  26. Banerjee, P. S., Ma, J., and Hart, G. W. (2015) Diabetes-associated dysregulation of O-GlcNAcylation in rat cardiac mitochondria. *Proc. Natl. Acad. Sci. U. S. A.* **112**, 6050–6055
  27. Hu, C. M., Tien, S. C., Hsieh, P. K., Jeng, Y. M., Chang, M. C., Chang, Y. T., *et al.* (2019) High glucose triggers nucleotide imbalance through O-GlcNAcylation of key enzymes and induces KRAS mutation in pancreatic cells. *Cell Metab.* **29**, 1334–1349.e10
  28. Liu, F., Shi, J., Tanimukai, H., Gu, J., Gu, J., Grundke-Iqbal, I., *et al.* (2009) Reduced O-GlcNAcylation links lower brain glucose metabolism and tau pathology in Alzheimer's disease. *Brain* **132**, 1820–1832
  29. Balana, A. T., Mukherjee, A., Nagpal, H., Moon, S. P., Fierz, B., Vasquez, K. M., *et al.* (2021) O-GlcNAcylation of high mobility group box 1 (HMGB1) alters its DNA binding and DNA damage processing activities. *J. Am. Chem. Soc.* **143**, 16030–16040
  30. Shin, H., Cha, H. J., Na, K., Lee, M. J., Cho, J. Y., Kim, C. Y., *et al.* (2018) O-GlcNAcylation of the tumor suppressor FOXO3 triggers aberrant cancer cell growth. *Cancer Res.* **78**, 1214–1224
  31. Wang, T., Yu, Q., Li, J., Hu, B., Zhao, Q., Ma, C., *et al.* (2017) O-GlcNAcylation of fumarase maintains tumour growth under glucose deficiency. *Nat. Cell Biol.* **19**, 833–843
  32. Seo, H. G., Kim, H. B., Yoon, J. Y., Kweon, T. H., Park, Y. S., Kang, J., *et al.* (2020) Mutual regulation between OGT and XIAP to control colon cancer cell growth and invasion. *Cell Death Dis.* **11**, 815
  33. Shen, A., Kamp, H. D., Grundling, A., and Higgins, D. E. (2006) A bifunctional O-GlcNAc transferase governs flagellar motility through anti-repression. *Genes Dev.* **20**, 3283–3295
  34. Su, C., and Schwarz, T. L. (2017) O-GlcNAc transferase is essential for sensory neuron survival and maintenance. *J. Neurosci.* **37**, 2125–2136
  35. Lee, B. E., Kim, H. Y., Kim, H. J., Jeong, H., Kim, B. G., Lee, H. E., *et al.* (2020) O-GlcNAcylation regulates dopamine neuron function, survival and degeneration in Parkinson disease. *Brain* **143**, 3699–3716
  36. Yang, Y., Fu, M., Li, M. D., Zhang, K., Zhang, B., Wang, S., *et al.* (2020) O-GlcNAc transferase inhibits visceral fat lipolysis and promotes diet-induced obesity. *Nat. Commun.* **11**, 181
  37. Hardiville, S., Banerjee, P. S., Selen Alpergin, E. S., Smith, D. M., Han, G., Ma, J., *et al.* (2020) TATA-box binding protein O-GlcNAcylation at T114 regulates formation of the B-TFIIID complex and is critical for metabolic gene regulation. *Mol. Cell* **77**, 1143–1152.e7
  38. Ranuncolo, S. M., Ghosh, S., Hanover, J. A., Hart, G. W., and Lewis, B. A. (2012) Evidence of the involvement of O-GlcNAc-modified human RNA polymerase II CTD in transcription *in vitro* and *in vivo*. *J. Biol. Chem.* **287**, 23549–23561
  39. Lewis, B. A., Burlingame, A. L., and Myers, S. A. (2016) Human RNA polymerase II promoter recruitment *in vitro* is regulated by O-linked N-acetylglucosaminyltransferase (OGT). *J. Biol. Chem.* **291**, 14056–14061
  40. Deplus, R., Delatte, B., Schwinn, M. K., Defrance, M., Méndez, J., Murphy, N., *et al.* (2013) TET2 and TET3 regulate GlcNAcylation and H3K4 methylation through OGT and SET1/COMPASS. *EMBO J.* **32**, 645–655
  41. Feng, Q., Wang, H., Ng, H. H., Erdjument-Bromage, H., Tempst, P., Struhl, K., *et al.* (2002) Methylation of H3-lysine 79 is mediated by a new family of HMTases without a SET domain. *Curr. Biol.* **12**, 1052–1058
  42. Zhu, B., Chen, S., Wang, H., Yin, C., Han, C., Peng, C., *et al.* (2018) The protective role of DOT1L in UV-induced melanomagenesis. *Nat. Commun.* **9**, 259
  43. Kim, W., Kim, R., Park, G., Park, J.-W., and Kim, J.-E. (2012) Deficiency of H3K79 histone methyltransferase Dot1-like protein (DOT1L) inhibits cell proliferation. *J. Biol. Chem.* **287**, 5588–5599
  44. Ishiguro, K., Kitajima, H., Niinuma, T., Ishida, T., Maruyama, R., Ikeda, H., *et al.* (2019) DOT1L inhibition blocks multiple myeloma cell proliferation by suppressing IRF4-MYC signaling. *Haematologica* **104**, 155–165
  45. Franz, H., Villarreal, A., Heidrich, S., Videm, P., Kilpert, F., Mestres, I., *et al.* (2019) DOT1L promotes progenitor proliferation and primes neuronal layer identity in the developing cerebral cortex. *Nucleic Acids Res.* **47**, 168–183
  46. Leon, K. E., Buj, R., Lesko, E., Dahl, E. S., Chen, C.-W., Tangudu, N. K., *et al.* (2021) DOT1L modulates the senescence-associated secretory phenotype through epigenetic regulation of IL1A. *J. Cell Biol.* **220**, e202008101
  47. Cao, K., Ugarenko, M., Ozark, P. A., Wang, J., Marshall, S. A., Rendleman, E. J., *et al.* (2020) DOT1L-controlled cell-fate determination and transcription elongation are independent of H3K79 methylation. *Proc. Natl. Acad. Sci. U. S. A.* **117**, 27365–27373
  48. Okada, Y., Feng, Q., Lin, Y., Jiang, Q., Li, Y., Coffield, V. M., *et al.* (2005) hDOT1L links histone methylation to leukemogenesis. *Cell* **121**, 167–178
  49. Nguyen, A. T., Xiao, B., Neppl, R. L., Kallin, E. M., Li, J., Chen, T., *et al.* (2011) DOT1L regulates dystrophin expression and is critical for cardiac function. *Genes Dev.* **25**, 263–274
  50. Cho, M. H., Park, J. H., Choi, H. J., Park, M. K., Won, H. Y., Park, Y. J., *et al.* (2015) DOT1L cooperates with the c-Myc-p300 complex to epigenetically derepress CDH1 transcription factors in breast cancer progression. *Nat. Commun.* **6**, 7821
  51. Vlaming, H., McLean, C. M., Korthout, T., Alemdehy, M. F., Hendriks, S., Lancini, C., *et al.* (2019) Conserved crosstalk between histone deacetylation and H3K79 methylation generates DOT1L-dose dependency in HDAC1-deficient thymic lymphoma. *EMBO J.* **38**, e101564
  52. Vatahalli, R., Sagar, V., Rodriguez, Y., Zhao, J. C., Unno, K., Pamarthy, S., *et al.* (2020) Histone methyltransferase DOT1L coordinates AR and MYC stability in prostate cancer. *Nat. Commun.* **11**, 4153
  53. De Roover, A., Nunez, A. E., Cornelis, F. M., Cherifi, C., Casas-Fraile, L., Sermon, A., *et al.* (2021) Hypoxia induces DOT1L in articular cartilage to protect against osteoarthritis. *JCI Insight* **6**, e150451
  54. Kim, S. K., Jung, I., Lee, H., Kang, K., Kim, M., Jeong, K., *et al.* (2012) Human histone H3K79 methyltransferase DOT1L protein [corrected] binds actively transcribing RNA polymerase II to regulate gene expression. *J. Biol. Chem.* **287**, 39698–39709
  55. Wu, A., Zhi, J., Tian, T., Cihan, A., Cevher, M. A., Liu, Z., *et al.* (2021) DOT1L complex regulates transcriptional initiation in human erythroleukemic cells. *Proc. Natl. Acad. Sci. U. S. A.* **118**, e2106148118
  56. Deng, R.-P., He, X., Guo, S.-J., Liu, W.-F., Tao, Y., and Tao, S.-C. (2014) Global identification of O-GlcNAc transferase (OGT) interactors by a human proteome microarray and the construction of an OGT interactome. *Proteomics* **14**, 1020–1030
  57. Chen, Q., Chen, Y., Bian, C., Fujiki, R., and Yu, X. (2013) TET2 promotes histone O-GlcNAcylation during gene transcription. *Nature* **493**, 561–564
  58. Yu, S.-H., Boyce, M., Wands, A. M., Bond, M. R., Bertozzi, C. R., and Kohler, J. J. (2012) Metabolic labeling enables selective photocrosslinking of O-GlcNAc-modified proteins to their binding partners. *Proc. Natl. Acad. Sci. U. S. A.* **109**, 4834–4839
  59. Branon, T. C., Bosch, J. A., Sanchez, A. D., Udeshi, N. D., Svinkina, T., Carr, S. A., *et al.* (2018) Efficient proximity labeling in living cells and organisms with TurboID. *Nat. Biotechnol.* **36**, 880–887
  60. Ma, J., Hou, C., Li, Y., Chen, S., and Wu, C. (2021) OGT protein interaction network (OGT-PIN): a curated database of experimentally identified interaction proteins of OGT. *Int. J. Mol. Sci.* **22**, 9620
  61. Lazarus, M. B., Jiang, J., Kapuria, V., Bhuiyan, T., Janetzko, J., Zandberg, W. F., *et al.* (2013) HCF-1 is cleaved in the active site of O-GlcNAc transferase. *Science* **342**, 1235–1239

## Dot1L regulates histone O-GlcNAcylation

62. Lee, J.-S., and Zhang, Z. (2016) O-linked N-acetylglucosamine transferase (OGT) interacts with the histone chaperone HIRA complex and regulates nucleosome assembly and cellular senescence. *Proc. Natl. Acad. Sci. U. S. A.* **113**, E3213–E3220
63. Stephen, H. M., Praissman, J. L., and Wells, L. (2021) Generation of an interactome for the tetratricopeptide repeat domain of O-GlcNAc transferase indicates a role for the enzyme in intellectual disability. *J. Proteome Res.* **20**, 1229–1242
64. Alerasool, N., Segal, D., Lee, H., and Taipale, M. (2020) An efficient KRAB domain for CRISPRi applications in human cells. *Nat. Methods* **17**, 1093–1096
65. Valencia-Sánchez, M. I., De Ioannes, P., Wang, M., Vasilyev, N., Chen, R., Nudler, E., *et al.* (2019) Structural basis of Dot1L stimulation by histone H2B lysine 120 ubiquitination. *Mol. Cell* **74**, 1010–1019.e6
66. Worden, E. J., Hoffmann, N. A., Hicks, C. W., and Wolberger, C. (2019) Mechanism of cross-talk between H2B ubiquitination and H3 methylation by Dot1L. *Cell* **176**, 1490–1501.e12
67. Yang, X., Zhang, F., and Kudlow, J. E. (2002) Recruitment of O-GlcNAc transferase to promoters by corepressor mSin3A: coupling protein O-GlcNAcylation to transcriptional repression. *Cell* **110**, 69–80
68. Jínek, M., Rehwinkel, J., Lazarus, B. D., Izaurralde, E., Hanover, J. A., and Conti, E. (2004) The superhelical TPR-repeat domain of O-linked GlcNAc transferase exhibits structural similarities to importin alpha. *Nat. Struct. Mol. Biol.* **11**, 1001–1007
69. Levine, Z. G., Fan, C., Melicher, M. S., Orman, M., Benjamin, T., and Walker, S. (2018) O-GlcNAc transferase recognizes protein substrates using an asparagine ladder in the tetratricopeptide repeat (TPR) superhelix. *J. Am. Chem. Soc.* **140**, 3510–3513
70. Clarke, A. J., Hurtado-Guerrero, R., Pathak, S., Schüttelkopf, A. W., Borodkin, V., Shepherd, S. M., *et al.* (2008) Structural insights into mechanism and specificity of O-GlcNAc transferase. *EMBO J.* **27**, 2780–2788
71. Cheung, W. D., Sakabe, K., Housley, M. P., Dias, W. B., and Hart, G. W. (2008) O-linked beta-N-acetylglucosaminyltransferase substrate specificity is regulated by myosin phosphatase targeting and other interacting proteins. *J. Biol. Chem.* **283**, 33935–33941
72. Iyer, S. P. N., and Hart, G. W. (2003) Roles of the tetratricopeptide repeat domain in O-GlcNAc transferase targeting and protein substrate specificity. *J. Biol. Chem.* **278**, 24608–24616
73. Liu, L., Li, L., Ma, C., Shi, Y., Liu, C., Xiao, Z., *et al.* (2019) GlcNAcylation of Thr/Ser in short-form -GlcNAc transferase (sOGT) regulates its substrate selectivity. *J. Biol. Chem.* **294**, 16620–16633
74. Riu, I.-H., Shin, I.-S., and Do, S.-I. (2008) Sp1 modulates ncOGT activity to alter target recognition and enhanced thermotolerance in *E. coli*. *Biochem. Biophys. Res. Commun.* **372**, 203–209
75. Henikoff, S., Henikoff, J. G., Kaya-Okur, H. S., and Ahmad, K. (2020) Efficient chromatin accessibility mapping *in situ* by nucleosome-tethered tagmentation. *Elife* **9**, e63274